

## Induction Logging in Diverse Borehole Environments in the Elephant Field, Libya

Peter Elkington\* and Christopher Skelt\*\*

### قياسات المقاومة التأثيري في حفرة البئر متعدد البيئات في حقل الفيل بليبيا

بيتر ألكينجتون وكريستوفر سكيلت

إن قياس المقاومة التأثيري الذي يجري في الآبار المحفورة باستخدام طين زيتي القاعدة يبين باستمرار أدلة على غزو سوائل الرشح. حساب قطر الغزو باستخدام لوحة الترنادو التقليدية يحتاج إلى قراءات مدخلة للمقاومة الضحلة باستخدام أجهزة المقاومة الدقيقة كقياس المقاومة المستعرض الدقيق، ولكن هذه القراءات أو القياسات غير متوفرة في حفرة البئر الذي يستخدم فيه وسط عازل. التقنية الجديدة التي تستخدم قياس المقاومة التأثيري بمفرده، رغم كونها بسيطة ومتينة، إلا أنها تحاصر هذه المشكلة.

لقد طبقت هذه التقنية أو استخدمت كذلك على بيانات من آبار محفورة بواسطة طينة موصلة. وفي هذه الحالة فإن جزءاً من قيمة من الإشارة الكلية قد يكون بسبب بيئة حفرة البئر، وهذا يتطلب استرجاع هذا الجزء لأجل إستنتاج درجة التوصيل الكهربائي لصخور التكوين وهذا يظهر درجة الشك في المنحنيات المحسوبة والتي تزداد بنقصان مقاومة طينة الحفر. ونحن نحدد أو نقيس هذا بالنظر في القيم النسبية للإشارات التي سببها مشاركة صخور التكوين أو حفرة البئر.

هذه الطريقة لها - وعلى وجه الخصوص - تطبيقات في التكاوين منخفضة التوصيل الكهربائي حيث الإشارات ذات المدى المنخفض.

إن المعرفة المتداولة أو المعتادة والتي في الغالب اكتسبت من أجهزة الجيل الأول، تقول بأن القراءات التي قيمتها أكثر من مائة أو مائتين أو م-متر، هي غير دقيقة أو غير موثوق فيها.

إننا نبرهن بأنه بتعريض السرود الكهربائية لعمليات معالجة مناسبة، يمكن أن نثق في القراءات التي تصل على الأقل إلى 1000 أو م-متر. وهذا قد ساعدنا على تمييز أماكن الزيت ذات المياه العذبة بالتكوين الجيولوجي.

هذه التقنية لها تطبيقات حيثما الجيوب البيئية التي يتم فيها التطابق بين قياسات المقاومة التأثيري والمستعرض أثناء تعود التيار على اختيار واحد ويرفض الآخر.

إن أفضل فهم لطريقة عمل جهاز قياس المقاومة التأثيري في التكاوين عالية المقاومة يساعد في شرح التضارب الواضح بين القياسات التي على هيئة خواص حقيقية للتكوين كما هو الحال في الخواص المتباينة حسب الاتجاه أو الانحرافات عن مظهر الغزو أو الغمر التدريجي.

**Abstract:** induction logs run in wells drilled with oil based mud frequently show evidence of filtrate invasion. Computing diameter of invasion from a

traditional tornado chart requires input from a shallow reading resistivity device such as a microlaterolog, but these are not available in non-conductive boreholes. A new technique using induction measurements alone circumvents the problem, while being both simple and robust.

\* Reeves Technologies, Loughborough, U.K.

\*\* Lasmo plc, London, U.K.

*The technique has also been applied to data from wells drilled with conductive muds. In these cases, a significant part of the total signal can be due to the borehole environment, and this must be backed-out in order to derive the formation conductivity. This introduces a degree of uncertainty in the computed curves that increases as the mud resistivity decreases. We quantify this by looking at the relative magnitudes of signals due to formation and borehole contributions.*

*The approach has particular application in low conductivity formations where signals are of low amplitude. Conventional wisdom, largely inherited from first generation tools, is that readings greater than one or two hundred ohm-m are unreliable. We demonstrate that, subject to appropriate processing, logs can be trusted to at least 1000 ohm-m. This has helped us characterise an oil reservoir with fresh formation water.*

*The technique has application where the environmental envelopes of laterolog and induction measurements overlap, and where current practice is usually to select one and reject the other. A better understanding of induction tool performance in highly resistive formations helps explain apparent discrepancies between the measurements in terms of real formation properties such as anisotropy or deviations from step invasion profile.*

## INTRODUCTION

Resistivity logs are traditionally run to derive a value of true formation resistivity,  $R_f$ , in order to derive water saturation,  $S_w$ . The emphasis is, therefore, on obtaining accurate estimates for  $R_f$ , but this is not necessarily the most important formation property that can be derived from the logs.

We present two field examples where induction logs have been processed to optimise diameter of invasion and variations in conductivity close to zero conductivity. The traditional approach of selecting either laterolog or induction log, according to borehole and formation properties, was appropriate when the measurements were first introduced, but technical improvements have extended the overlap between the operating

envelopes of the two tool types. Although one of the two may be favoured, they are not mutually exclusive, and selecting only one can potentially deny the petrophysicist useful information about invasion and formation anisotropy. It is, therefore, worthwhile developing techniques to exploit the advances in logging tool technology.

Wells in which formation water is fresher than filtrate are often logged with induction alone. The borehole environment and radial resistivity profile encountered in the water legs are appropriate for deriving an accurate estimate of formation and water resistivity to apply in the hydrocarbon zones. However, the large increase in resistivity in hydrocarbon zones alters the radial resistivity profile so that resistivity increases with distance from the borehole, which favours the laterolog. The techniques we present here for working with induction logs in unfavourable environments are relevant to these frequently encountered circumstances.

### Extending the Low Conductivity Limit

Formation resistivities in the reservoir of the Elephant field in Libya extend up to thousands of ohm-metres. Core analysis suggests that this is due to the formation becoming progressively more oil wet with increasing height above the contact. This is supported by the very low water saturations computed by the Archie equation applied to the highest resistivities.

While these high resistivities are easily measured by laterologs, they present a challenge for induction logs run in wells drilled with oil based mud. In these circumstances the priority switches from deriving a resistivity for use in saturation determination to optimising the description of the lowest conductivities with the aim of detecting small variations resulting from wettability changes.

The measurement accuracy for modern induction tools is claimed to be better than 0.001 S/m, which implies that computed resistivity logs should be accurate up to 1000 ohm-m. However, conventional wisdom is that induction logs are unreliable at formation resistivities above a few hundred ohm-metres, and that laterologs are preferred in these circumstances. The combination

of a massive high resistivity oil-filled sand and oil-based mud in the F3 well provide an opportunity to test the low conductivity limit of the tool's response.

**Low Conductivity Signal Compression**

The F3 logs are shown in figure 1. Curves in the rightmost track were processed using field default parameters. Field processing includes a curve "squasher" that prevents negative conductivities (from near-borehole conductive or magnetic anomalies) being displayed on a logarithmic resistivity grid. The process compresses displayed conductivity values progressively below a low conductivity threshold whose default value is 0.005 S/m (equivalent to 200 ohm-m). The effect of removing the squasher is also shown in figure 1.

The highest resistivities now approach 2,000 ohm-m with no obvious degradation in character, evidence that supports the claimed measurement accuracy. It is now possible to identify a change in the resistivity gradient close to x235 ft, at about the elevation above the contact thought to be associated with the onset of mixed and oil wet conditions. We conclude that the default display is unduly conservative in this favourable borehole environment.

**Induction Log Borehole Effects**

The apparent conductivity  $\sigma_a$  seen by an induction tool transmitter-receiver coil array is given by

$$\sigma_a = g\sigma_m + (1-g)\sigma_f \tag{1}$$

where  $g$  is an integrated radial geometric factor, and  $\sigma_m$  and  $\sigma_f$  are mud and formation conductivities respectively.

The magnitude of  $g$  tells us how much borehole correction has been applied, but is not necessarily a good indication of the size of the borehole effect. This is because  $g$  is determined under static conditions - it ignores the dynamic component of borehole effect arising from interactions between a moving tool and a non-constant hole environment. In low conductivity borehole fluids, the dynamic component can be ignored, but it becomes progressively more significant as the fluid conductivity increases.

Dynamic borehole effects constitute a source of noise that is inherently difficult to quantify, let alone remove. Nevertheless, they provide a framework for quantifying confidence levels for high resistivity values from real-world induction logs.

We cannot easily quantify all the individual sources of borehole-related noise and their complex interactions. It is reasonable to say, however, that as the size of the nominal borehole correction increases relative to the formation signal we are trying to extract, confidence in the computed formation signal will decrease. For example, we consider the situation of equal borehole and formation signal magnitudes.

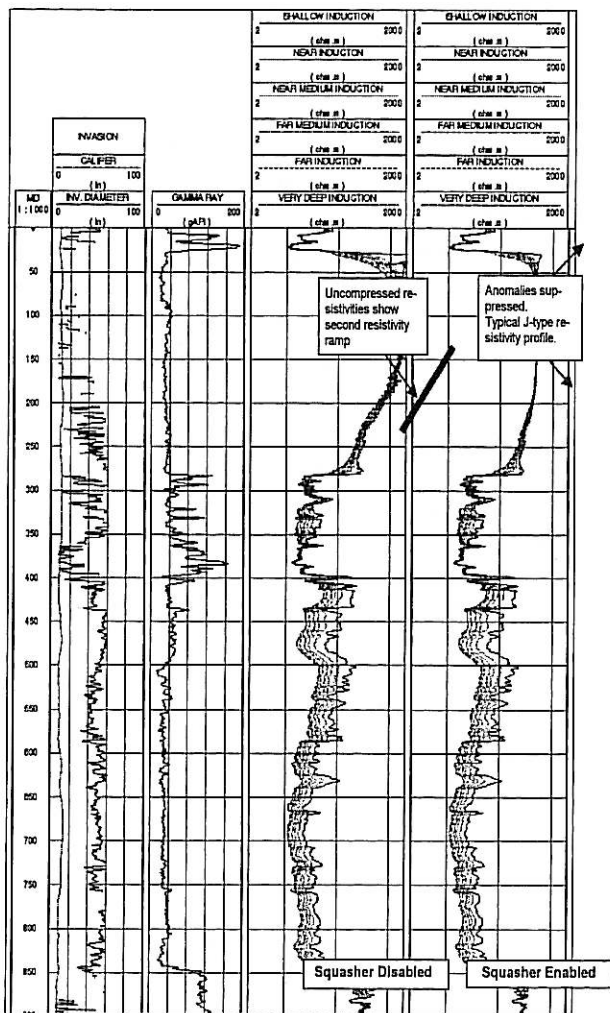


Fig. 1. Induction log low conductivity response, well F3.

From equation (1), for a single coil pair or sub-array the nominal signal due to the borehole is  $g_m$  and that due to the formation is  $(1-g)\sigma_f$ . These are equal when:

$$\frac{\sigma_f}{\sigma_m} = \frac{g}{(1-g)} \tag{2}$$

Each sub-array is a source of borehole-related noise. Let us assume that the statistical distributions of the noise are independent, then the noise in any of the composite curves (such as the Deep and Medium, or other derived curve) is derived by taking a weighted RMS average of the individual sub-array noise levels. The weights are those used in the computation of the derived curves from the individual sub-arrays.

Figure 2 shows  $R_t/R_m$  as a function of bit size and standoff for deep and Medium curves processed from the array induction tool, for the condition of formation signal equal to nominal borehole signal. Scaling the condition (for example, borehole signal equal to 200% of

formation signal) scales the maximum  $R_t/R_m$  value, but does not change the curve order.

The practical interpretation of these curves is that they define resistivity envelopes above which borehole-related noise is likely to become intrusive. It does not mean that higher values of resistivity are unusable, only that care needs to be exercised in their interpretation.

Indeed, it would be wrong to regard the curves in figure 2 as delineating upper limits for  $R_t/R_m$  without regard for other aspects of the borehole environment. For example, experience suggests that in good wellbore conditions (on-gauge hole, no caves),  $R_t/R_m$  interpreted from figure 2 is pessimistic by a factor of at least 2. Conversely, in cases of extreme rugosity and irregular hole enlargement, the figures indicate maximum  $R_t/R_m$  values that are optimistic by a similar factor.

### Invasion Diameter from the Array Induction

Well test results on a number of Elephant appraisal wells indicated high skin. A possible explanation was that the perforations had not penetrated beyond the zone damaged by filtrate in this hard formation. This put a high priority on determining diameter of invasion  $D_i$ , normally considered a by-product of true formation resistivity determination. Estimates of invasion diameter from laterolog and induction can be compared in the F2 well.

Diameter of invasion is defined in terms of the commonly assumed step invasion profile, and is normally computed as part of a tornado chart calculation. This chart allows the three step profile parameters  $R_t$ ,  $R_{xo}$  and  $D_i$  to be computed from three input curves, normally two induction curves plus a shallow reading laterolog curve. In non-conductive borehole fluids, the laterolog curve is not available. The whole chart changes as a function of  $R_{xo}$  because of skin effect.

Although F2 contained conductive borehole fluid, we choose to use a technique for  $D_i$  determination that could also be applied to wells with non-conductive fluids. Our new method is set in the conductivity domain.

The new solution for  $D_i$  is derived from geometric factor theory. The apparent

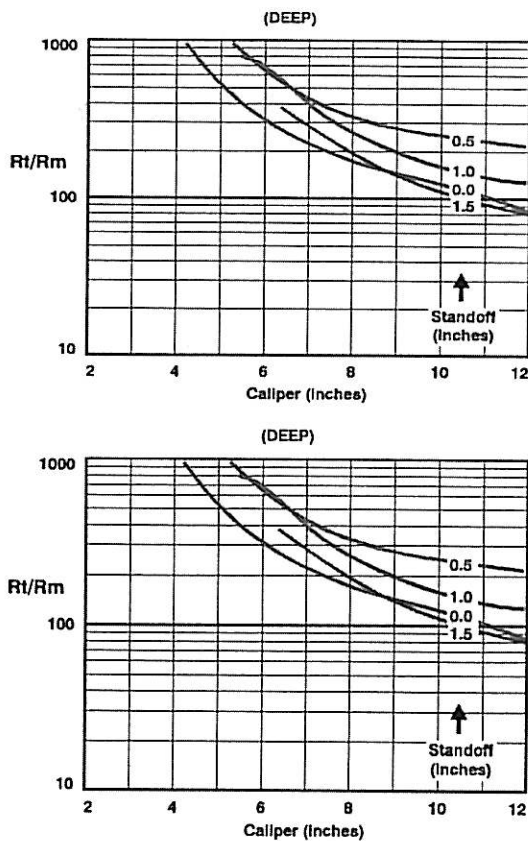


Fig. 2. Deep and medium curve signal to noise indicators. The curves connect points for which borehole and formation signals are of equal magnitude.

conductivities from two differently spaced induction arrays for the case of step profile are:

$$\begin{aligned} \sigma_1 &= g_1 \sigma_{xo} + (1-g_1) \sigma_t \\ \sigma_2 &= g_2 \sigma_{xo} + (1-g_2) \sigma_t \end{aligned}$$

where  $g_1$  and  $g_2$  are integrated radial geometric factors corresponding to particular values of  $D_i$ . Taking differences, we get:

$$(\sigma_2 - \sigma_1) = \sigma_{xo} (g_2 - g_1) + \sigma_t (g_1 - g_2)$$

Re-arranging we get:

$$(\sigma_2 - \sigma_1) = (g_2 - g_1) (\sigma_{xo} - \sigma_t) \tag{3}$$

Adding a third measurement, and taking a second difference gives:

$$(\sigma_3 - \sigma_1) = (g_3 - g_1) (\sigma_{xo} - \sigma_t) \tag{4}$$

Dividing equation (4) by equation (3) eliminates  $\sigma_{xo}$  and  $\sigma_t$ :

$$\frac{\sigma_3 - \sigma_1}{\sigma_2 - \sigma_1} = \frac{g_3 - g_1}{g_2 - g_1} \tag{5}$$

If we ignore skin effect, the geometric factors in equation 6.3 depend solely on  $D_i$ . Moreover, apparent conductivity data from all invasion profiles with fixed  $D_i$  must appear on a straight line on a plot of  $(\sigma_3 - \sigma_1)$  against  $(\sigma_2 - \sigma_1)$ . This has been tested by crossplotting data generated from analytical models. Figure 3(a) is a plot of the conductivity difference  $(\sigma_3 - \sigma_4)$  against  $(\sigma_2 - \sigma_3)$  using data from the  $R_t > R_{xo}$  tornado chart. It is striking that the  $D_i$  values fall on almost perfect straight lines pointing to the origin, consistent with equation (5) the data points within each line correspond to different values of  $R_t/R_{xo}$ . This data set was generated for  $R_{xo} = 1$  ohm-m, and does, in fact, include skin effect.

The conductivity difference plots suggests a simple and robust method for extracting  $D_i$  information from array induction logs. Straight lines that pass through the origin of the conductivity difference graphs are defined solely by their gradients. In the case of figure 3(a), this is simply  $(\sigma_2 - \sigma_3) / (\sigma_3 - \sigma_4)$ . This is plotted as a function of  $D_i$  in figure 3(b). Each point is actually a cluster of data values that span  $R_{xo}/R_t$  values of

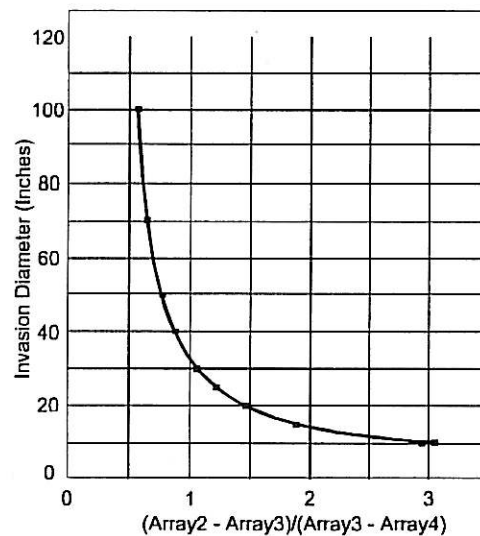
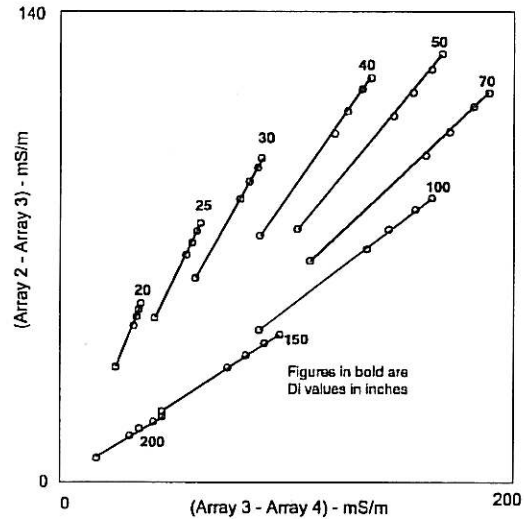


Fig. 3 (top). Computer model results showing points of equal  $D_i$  fall close to straight lines on plots of conductivity differences. Fig. 3 (bottom). Slopes of the lines in figure 3 (top) are plotted as a function of  $D_i$ . The model results exhibit that  $D_i$  values computed in this way do not depend strongly on  $R_{xo}$ .

0.4, 0.15, 0.1, 0.05, 0.025, 0.02 and 0.01. It is apparent, therefore, that the function is practically independent of  $R_t/R_{xo}$ .

Using this method,  $D_i$  values were computed for the F2 well, and compared with those computed from a dual laterolog / microlaterolog combination run in the same well. F2 was drilled with an 8.5 inch (216 mm) bit and water based mud with  $R_m$  at bottom hole temperature of 0.39 ohm-m. The induction was run with 1.5 inch (38 mm) standoffs.

The analysis in figure 4 suggests these conditions are unfavourable for the induction tool

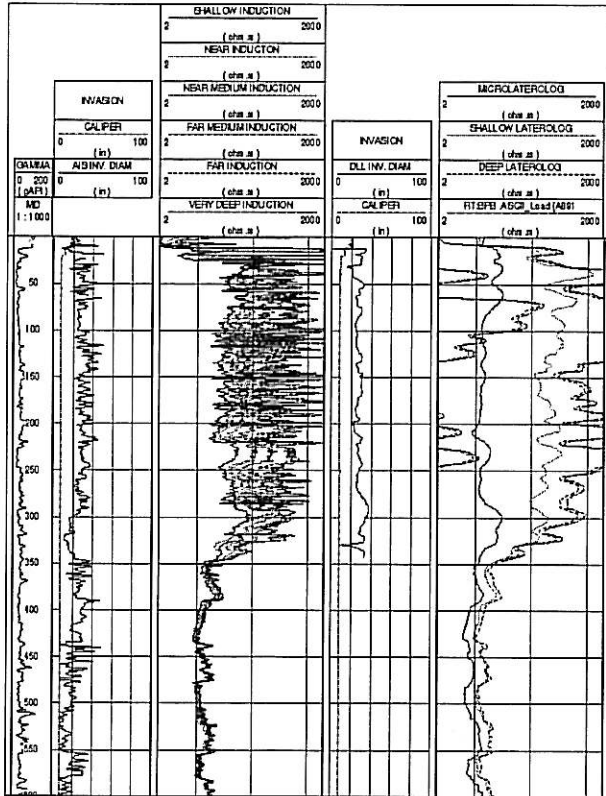


Fig. 4. Array Induction and Dual Laterolog data sets from the F2 well. The borehole environment was unfavourable for induction logs, but  $D_i$  estimates generated from conductivity differences were stable, and comparable to those from laterologs.

over the oil leg, where the laterologs record high to very high values of  $R_p$ . This is reflected in the character of the induction curves, which appear to be very sensitive to small variations in hole quality and tool position when viewed on a resistivity scale. In the conductivity domain, however, the induction curves are much less active, and differences between induction curves are reasonably consistent. The  $D_i$  curve computed from conductivity differences is correspondingly stable, and in approximate agreement with that from the laterologs. The agreement suggests that the actual invasion profile may be step-like and that the method yields valid results.

## CONCLUSIONS

The quality of induction log data in high  $R_p/R_m$  environments can be assessed by comparing signal amplitudes originating in formation and borehole regions. Where induction log borehole signals are small, for example in non-conductive environments, attention can usefully be paid to the parameters controlling the processing of low

conductivity values in order to avoid unnecessary cosmetic distortion.

Invasion diameter values can be computed from the conductivity differences available from array induction tools even in unfavourable environments. The method is simple, independent of the  $R_t$  computation yields results similar to those obtained with laterologs.

## ACKNOWLEDGEMENTS

The authors would like to thank the Libyan National Oil Corporation and partners for data release. The logs were acquired by Geoservices Logging Libya.

## REFERENCES

- Martin, D.W., Spencer, M. C., and Patel, H.K. , 1984. The digital induction - a new approach to improving the response of the induction measurement. *Trans. SPWLA*, paper M
- Patniyot, S., 1985. True resistivity and depth of invasion study - an approximation method based on pseudo - geometrical factors. *Trans. SPWLA*, paper ZZ.
- Howard, A. Q. , 1992. A new invasion model for resistivity log interpretation. *Log Analyst* **33** (2), 96-110.